Electron Transfer in the P450cam/PDX Complex. The QM/MM e-Pathway†

Frank Wallrapp,‡ Diego Masone,§ and Victor Guallar*

ICREA Research Professor, Life Science Department, Barcelona Supercomputing Center, Jordi Girona, 29, 08034 Barcelona, Spain

Received: April 23, 2008; Revised Manuscript Received: June 30, 2008

Electron transfer processes are simple but crucial reactions in biochemistry, being one of the main steps in almost all enzymatic cycles. Obtaining an atomic description of the transfer pathway is a difficult task, at both the experimental and theoretical levels. Here we combine protein−protein docking algorithms, protein structure prediction methodologies and mixed quantum mechanics/molecular mechanics techniques to map the electron transfer pathway between cytochrome P450 camphor and its redox partner, putidaredoxin. Although the mechanism of interaction and electron transfer for this redox couple has been under investigation for over 30 years, the exact mechanism and electron transfer pathway has not been fully understood, yet. Our results report the first ab initio quantum chemistry description of the electron migration. The obtained electron transfer pathway indicates the key role of Arg112 of P450 and Asp38 of PDX and the existence of slightly different electron transfer pathways for different protein−protein complexes.

I. Introduction

The electron transfer process is one of the simplest but most crucial reactions in biochemistry, being one of the main step in almost all enzymatic cycles.[1,2] It might involve a relative short pathway, for example, from a substrate or cofactor directly bound in the vicinity of the acceptor group, or rather large electron transfer pathways, for example across protein−protein complexes, where the donor and acceptor might be considerably apart from each other. In any of these cases getting direct information of the electron pathway is not a trivial task. Such atomic and electronic detailed information, however, is very valuable in terms of a better understanding of the enzymatic cycle, which might lead, for example, into more efficient protein inhibitor design.

The usual experimental procedure to determine the electron transfer pathway is by means of direct protein mutation. Although this technique can probe the importance of some residues in the electron migration, it can bring secondary effects like structural changes or significant perturbation of the electrostatics, which might mask the real cause for the loss/gain of electron conductivity. Computational tools offer an alternative approach that might reduce the time and expenses of further experimental work to map the electron transfer pathway. They do not introduce any perturbation on the system and have the spatial and temporal resolution needed. They require, however, a fair resolution crystal structure to start with, a crystal that should be close in conformational space to the active structure. Currently, there are various programs capable of obtaining an approximate electron transfer pathway. They are based on topological search algorithms finding the shortest pathways between the defined electron donor and acceptor[3] or on approximate semiempirical extended Hückel level of theory,[4−6] for instance. The current increase in computational resources, together with the recent development of mixed quantum mechanics/molecular mechanics (QM/MM) algorithms, however, allow us to design more rigorous methodologies capable of tracking the electron delocalization.[7−10] Current computational resources, for example 8 processors on a SGI-Altix cluster, allow performing a wave function analysis for a large quantum region, on the order of 400 atoms, in about 1−2 days.

The family of cytochrome P450 monooxygenases (P450) is ubiquitous in human biology, playing a key role in the metabolism of pharmaceutical agents and other ingested exogenous compounds.[11,12] These enzymes insert an oxygen atom from O_2 into a wide variety of substrates, with substrate specificity determined by the nature of the protein active site cavity. The first catalytic step from the low-spin resting state involves camphor binding, which displaces the water molecule from the heme pocket. This binding produces a shift from low-to-high spin, accompanied by a 130 mV increase in the reduction potential, which allows thermodynamic reduction by putidaredoxin (PDX).[13−15] The crystal structure of the P450-PDX complex has not yet been resolved. However, there are numerous studies on modeled complex structures.[16−18] The first model, proposed by Pochapsky et al., has a distance of 12.0 Å between the heme iron of P450cam and the iron of the Fe_2S_2 cluster in PDX closest to the surface.[16] Furthermore, it points out salt bridges from Arg109 (P450) to Asp34 (PDX), Arg112 (P450) to Asp38 (PDX) and Arg79 (P450) to Trp106 (PDX). The model proposed by Roitberg et al. is very similar, also having the distance of 12 Å between the two redox centers and salt bridges between the residue pairs mentioned above.[17] They determined both binding sites in performing electrostatic Poisson−Boltzmann calculations resulting in a triangle of continuous negative electrostatic potential between Asp34, Asp38 and Trp106 of PDX and patches of positive electrostatic potential contours in the proximal face of P450. They also obtained pathway models for the electron transfer by calculating the electron couplings of the surface residues to their respective redox center. The results strongly highlight Asp38 and Ser44 in PDX and Arg112 and Leu356 in P450 as possible electron transfer residues. In addition to theoretical calculations, they applied site mutagenesis experiments identifying Arg112 (P450) and Asp38 (PDX) as mayor residues responsible for binding and electron transfer,

† Part of the "Sason S. Shaik Festschrift".

* Corresponding author. E-mail: V.G., victor.guallar@bsc.es.
‡ E-mail: frank.wallrapp@bsc.es.
§ E-mail: diego.masone@bsc.es.

10.1021/jp803538u CCC: $40.75
Published on Web 09/30/2008

in agreement with previous mutagenesis studies.[19,20] Roitberg et al. propose an electron transfer pathway from the Fe_2S_2 cluster via Cys39 to Asp38 of PDX and making a protein−protein jump into Arg112 of P450 and from there a second through space jump to the propionate group of the heme in P450. They further point out a less probable electron transfer pathway through Ser44 (PDX) and Leu356 (P450).[17] Recent studies on P450-PDX also verify the salt bridge between Arg112 (P450) and Asp38 (PDX), whereas the existence of the previously suggested salt bridge between Tyr78 (P450) and Trp106 (PDX) [16,21] was not confirmed.[18,22] The two proposed complex structures have a similar iron−iron distance of 14.7 and 16.6 Å, but the second has PDX rotated about 90° around the vertical axis. Both complexes include a close contact of Arg112 (P450) and Asp38 (PDX) forming the predicted salt bridge. Recently, Harada et al. performed experiments with a "one-legged heme", where the 6-propionate side chain is replaced by a methyl group.[23] The enzymatic activity of the reconstituted P450cam, having this mutated heme, is maintained whereas PDX affinity is approximately 3.5-fold weaker. Their results indicate that the 6-propionate side chain of heme has mainly two roles, namely fixation of the PDX-binding site by the Arg112 residue and prevention of formation into the inactive P420 species in stabilizing the Fe-Cys357 ligation. The previous suggested electron transfer pathway through Arg112 into the heme propionates[17] could not be confirmed.

In this paper we present a QM-MM description of the electron transfer pathway. We use a novel QM/MM protocol recently developed by us where we can track the evolution of the spin density in the transfer region between the donor and the acceptor.[24] In QM/MM methods, the Schrödinger equation is only solved for those atoms included in the quantum region (QM region). The MM or classical region is described by a set of "solid" spheres with point charges. Electrons can only flow (or localize) between those atoms in the QM region. Thus, one can imagine multiple combinations of including/excluding residues in the QM region aiming to underline the pathway taken by the electron from the donor to the acceptor. The results clearly indicate the importance of Arg112 (P450) in the electron transfer pathway and the existence of slightly different electron transfer pathways for different protein−protein complexes.

II. Methods

Protein−Protein Docking. Protein Data Bank (PDB) structures 1DZ4 (ferric P450cam) and 1OQQ (C73S/C85S mutant of PDX) were taken for the calculations. The two mutations in 1OQQ were reversed using the PLOP code.[25,26] The protonation states of the histidines in P450 and PDX were assessed by visual inspection. In particular, only histidines 17, 270, 308, 347, 352 and 391 of P450 were protonated on the epsilon position and none were doubly protonated. Asp297 of P450 is protonated according to recent studies.[27−29] The actual docking was performed using the rigid-body docking program pyDock,[30] which uses electrostatics and desolvation energy to score docking poses generated with FT-dock.[31] We applied pyDock with the default parameter set including AMBER94 as the underlying force field. For further details we refer to the original paper. We used two sets of structures to run the protein−protein docking simulations. First, with PDX ignoring the iron−sulfur cluster and second, with PDX having the active site charge properly described, which includes a −2 charge from the Fe_2S_2 cluster. The iron−sulfur cluster is located in the surface of the protein and its large charge density might be crucial in the binding process.

Protein−Protein Refinement. To refine the protein−protein docking, we use our latest software PELE, which combines a steered stochastic approach with protein structure prediction methods.[32] PELE's heuristic algorithm is based on consecutive iteration of three main steps:

(1) Initial perturbation. The procedure begins with the generation of a local perturbation involving a translation and rotation of the center of mass of a ligand (in our case PDX).

(2) Side chain sampling. The algorithm proceeds by sampling all side chains in the interface using the algorithms designed by Jacobson et al.[25,33]

(3) Minimization. The last step in every move involves the minimization of a region including, at least, all residues local to the atoms involved in steps 1 and 2.

These three steps compose a move, which is accepted (defining a new minima) or rejected on the basis of a Metropolis criterion for a given temperature. The collection of accepted steps forms a stochastic trajectory. To produce a larger backbone response to the ligand translation and rotation, there is an option to include an additional perturbation on each α carbon. The α carbons might be displaced by following one of the lowest eigenvectors obtained in a anisotropic network model (ANM) approach, a simple model for normal-mode analysis.[34] As a part of the perturbation step, the system is also minimized with a harmonic constrained on each displaced α carbon. This combination of ligand and backbone perturbations, coupled to a side chain prediction and unconstrained minimization, results in a more effective exploration of the protein energy landscape, capable of reproducing conformational changes along the protein−protein adjustment migration. This is necessary due to the rigid nature of the protein−protein docking algorithm.

PELE uses the OPLS2005 force field and a generalized Born implicit solvent. PDX was randomly translated by 0.3 Å within each PELE cycle. Side chain sampling involved residues within a 3 Å vicinity of the protein−protein interface. After the side chain sampling, the minimization was applied to residues that are less than 4 Å away from the same interface. ANM steps were introduced every 3 PELE cycles and implied α carbon movements of 1 Å along an ANM vector randomly chosen from the lowest 6 modes. Within all steps both active sites were excluded to keep their original geometry. The 4 complex structures chosen for the electron transfer calculations were then solvated into a 10 Å shell of TIP3P water molecules and a short molecular dynamic water equilibration was performed using GROMACS.[35]

QM/MM. Mixed quantum mechanics/molecular mechanics (QM/MM) approaches have been created, which can join together a quantum and a classical representation of different sectors of a complex condensed phase system. The conjunction of these technologies contains the elements necessary to properly describe the potential energy surfaces relevant to enzymatic chemistry. The reactive region of the active site can be treated with a robust ab initio quantum mechanics (QM) methodology. The remainder of the protein can be modeled at the molecular mechanics (MM) level, providing the appropriate structural constraints and electrostatic and van der Waals interactions with the core reactive region.[36−40] All QM/MM calculations were performed with the QSite program.[41] We used the DFT B3LYP level of theory for the precursory QM/MM minimizations and further Hartree−Fock for the QM/MM single point energy calculations. Our findings indicate that Hartree−Fock localizes the electron better than DFT, which also correlates with other studies.[42] Both setups included the 6-31G* basis set and a lacvp pseudopotential for the iron center.

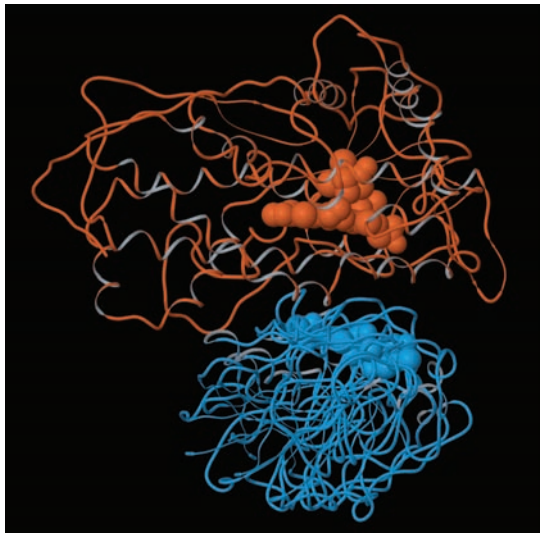

Figure 1. Representative structures of the best 10 docking results of P450 (brown) and PDX (blue) having explicit −2 charge on the active site of PDX. The heme group and the iron−sulfur cluster are shown in a spacefill representation.

QM/MM Electron Transfer Path Search Algorithm. The methodology we have designed consists of the following procedure.[24] First we proceed by building the parameters for the donor and the acceptor in the oxidized state. Therefore, the electron has left the donor but has not yet arrived to the acceptor. The parametrization consists in a QM/MM energy minimization of the donor and acceptor (both in the oxidized state) from which we extract the geometry and atomic charges from the electrostatic potential. This parametrization is important because in the next step of our procedure both residues will be included in the classical region. Thus, there is no electronic description of the donor and acceptor. Instead, we focus on the "transfer region" between them, the region that now contains the electron. After the parametrization we start an iterative process where we initially include the entire transfer region in the QM region of the QM/MM calculation, and perform a calculation where we add one electron and specify a doublet spin state. We are searching for the first receptor for the electron. Once we have located it, we proceed to the second iteration by turning the first identified residue into a classical residue, excluding it from the quantum region. By excluding this residue, we do not allow for an electronic description of it and the electron needs to find another host. In doing so, we now look for a second electron acceptor in the transfer region. We iterate this procedure until we find a direct pathway connecting the donor and the acceptor. For very large transfer regions, the procedure could be applied to several subregions, of approximately 400 atoms (the present limit for our current QM/MM methods) to cover the entire donor−acceptor distance. We name this procedure the QM/MM e-pathway.

III. Results

Protein/Protein Docking and Refinement. Representative structures of the best 10 docking results are shown in Figure 1. PDX is the smaller protein, which is being docked into the larger P450 protein. As seen in Figure 1, all structures bind to the commonly accepted binding site of PDX on the proximal face of P450. These results are in agreement with previous studies on P450-PDX binding.[16−18] We chose 15 structures with minimal distance between the redox sites and close Arg112 (P450) to Asp38 (PDX) contact out of the best 50 structures of pyDock for further structure refinements using PELE as described above. From there, according to minimal iron−iron distance and binding energy, a final set of four structures is taken for the electron transfer pathway calculations. The PDB structures are available upon request from the author. Within this set, complex 1, 3 and 4 are similar to the previously proposed complexes[16−18] forming salt bridges between Arg112 (P450) and Asp38 (PDX) and having iron−iron distances of 14.4, 12.7 and 15.7 Å, respectively. In complex 2, PDX is rotated about 180° around the vertical axis, thus having Asp38 turned away from Arg112. Here, the iron−iron distance is 14.2 Å. Karyakin et al. also proposed a second docking complex which has a rotation of PDX within similar range.[18] Figure S1 (Supporting Information) represents the top 10 structures when we neglect the charge in the active site of PDX. We see a dispersion of the binding region affecting different regions in the P450 surface. The important role of the electrostatics in the protein−protein recognition and binding has been underlined by previous studies.[17] Our results confirm this critical role of the electrostatics forces.

QM/MM Spin Density Validation. To validate the effects of the QM/MM boundaries in the spin densities, we performed full QM and QM/MM calculations on tripeptides (Ala-X-Ala) of all amino acids in the gas phase and in continuum solvent with two different dielectric constants, 2 and 80. We studied the two different boundary treatments that QSite allows, frozen orbitals and hydrogen atom caps (H-Cap). Using frozen orbitals for the QM/MM cut, results in 7 residues in a spin localization significantly different when compared to those from full QM. The frozen orbital method introduces an electron (and a MM counter charge) in a parametrized orbital right into the boundary region resulting in large effects in the molecular orbitals localized in the vicinity (1−2 bonds) of the boundary region. To work effectively, the frozen orbital should be placed in a region far away from the possible excess of electron localization. Thus, in an exploration technique like the one we are proposing here, this QM/MM boundary method does not seem to be a valid option. H-Cap cut, on the contrary, localizes the spin in good agreement with full QM calculations for all peptides if the H-Caps are not placed next to carbonyl groups. Figures S2−S7, showing the spin density plots of tyrosine and asparagine for QM, QM/MM H-Cap and QM/MM frozen orbital, are given in the Supporting Information. Using these findings, we exclusively applied H-Cap cuts and only after C_α or N in the backbone for the QM/MM calculations in the electron transfer pathway algorithm.

PDX-P450 Electron Transfer. We have calculated the electron transfer pathway for the four P450-PDX structures selected in the docking and refinement process. Within each iteration, the residue with the most electron affinity is determined, marked and excluded from the QM region for the next iteration. In our calculations, the electron did sometimes localize into residues forming "dead end" pathways, which do not connect both redox sites, or residues being far off any possible electron transfer pathway. An example therefore is shown in Figure 2 and will be discussed later. These findings do not have to be treated specifically as we only account residues to the final electron transfer pathway that are either directly connected through the backbone or lie in reasonable distance to each other. In particular, we are looking for through space jumps with a distance less than 5 Å. Thus, we iterate the process until we find the first connection between the donor and acceptor. The specific results on the four different complex structures are given in the following.

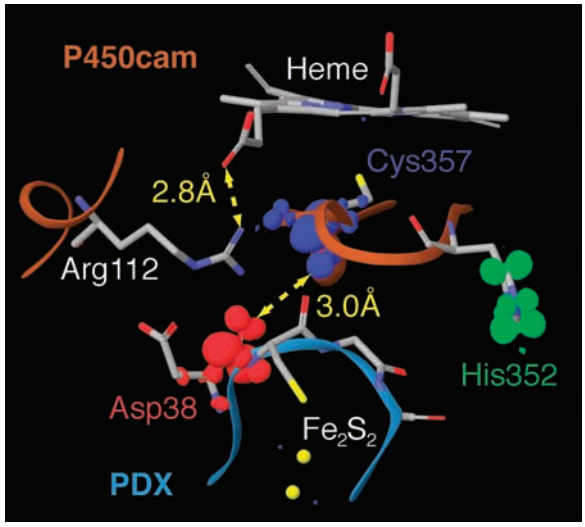

Figure 2. Electron transfer pathway for complex 1 of P450-PDX including the carbonyl group of Asp38 (PDX) and Cys357 (P450). His352 (P450), shown in green, gives an example of residues having high electron affinity but not lying on the electron transfer pathway between the iron−sulfur cluster and heme.

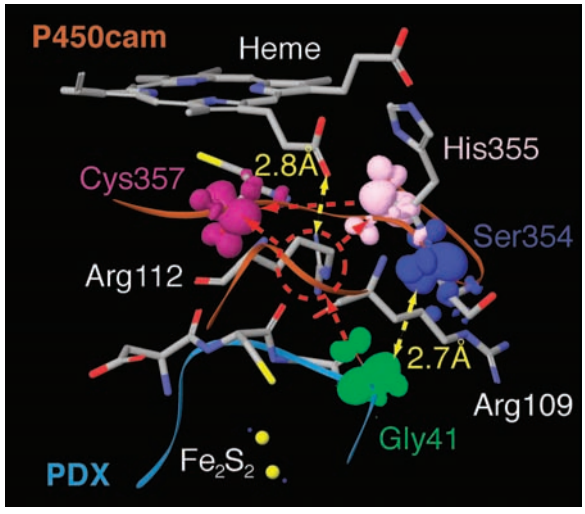

Figure 3. Electron transfer pathway for complex 2 of P450-PDX including the carbonyl groups of Gly41 (PDX), Ser354 (P450), His355 (P450) and Cys357 (P450). An alternative electron pathway of P450-PDX having Arg109 (P450) neutralized is highlighted in red.

Complex 1. Figure 2 shows the results of the calculations for the first complex structure. Our calculations result in spin density in the carbonyl groups of Asp38 of PDX (red) and Cys357 of P450 (blue). These two residues are in close contact of only 3 Å and, thus, can be easily bridged by the electron with a single through space jump. Both residues lie in direct vicinity to Arg112 (P450), which also forms a salt bridge to Asp38 (PDX). The figure further includes an example for residues having enough electron affinity to localize the electron but not being part of the actual electron transfer pathway as no further residues get marked forming a pathway including it. In this particular case, the residue is His352 of P450 with spin density in the side chain shown in green color.

Complex 2. Figure 3 shows the results of the calculations on the second complex structure. The spin densities identify an electron transfer pathway around Arg112 (P450). It starts at the carbonyl group of Gly41 in PDX (green), performs a protein−protein jump of about 2.7 Å to the carbonyl group of Ser354 (blue), already in the P450, and then follows the backbone up to Cys357 (violet). Keeping in mind that PDX is turned around its vertical axis, it is an interesting fact that the pathway does not go through Asp38 but Gly41 of PDX.

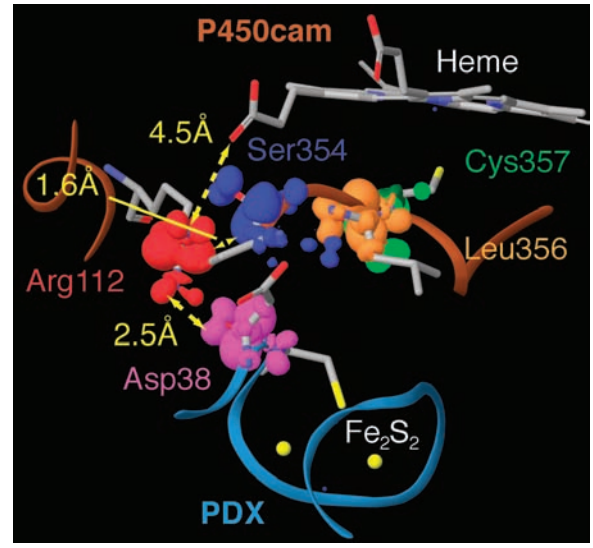

Figure 4. Electron transfer pathway for complex 3 of P450-PDX including the carbonyl group of Asp38 (PDX), the side chain of Arg112 (P450) and the carbonyl groups of Ser354, Leu356 and Cys357 of P450.

Complex 3. Figure 4 shows the spin densities of calculations on the third complex structure. Identified residues are Asp38 (violet) of PDX and Arg112 (red), Ser354 (blue), Leu356 (orange) and Cys357 (green) of P450. The electron transfer pathway includes the carbonyl group of Asp38 in PDX and moves to P450 through the side chain of Arg112, and the carbonyl groups of Ser354, Leu356 and Cys357. These residue form a pathway between the two redox sites with two short through space jumps, the first between Asp38 (PDX) and Arg112 (P450) of about 2.5 Å and the second between Arg112 and Ser354 (both P450) of about 1.6 Å.

Complex 4. Calculations on the fourth complex structure are shown in the Figure 5. Identified residues with spin density are Asp38 (green) of PDX and Arg112 (red) and Cys357 (blue) of P450. These findings specify an electron transfer pathway from Fe_2S_2 to Asp38 (PDX), jumping over to Arg112 on P450 with a distance of 2.8Å and performing a second through space jump of 2.2Å to Cys357 underneath the heme.

IV. Discussion

The active site of PDX, located near the surface, presents a large density of negative charge. In the core of the active site we find the iron−sulfur cluster, with a −2 charge in the reduced (predocking) state. In the immediate vicinity of the active site core, and pointing into solution, we find a negatively charged residue, Asp38, for a total active site charge of −3. On the other side, P450 has most of its surface negatively charged, with the exception of the putative binding site, the heme proximal face of the P450. To check for the importance of the electrostatic forces in the binding process, we have docked both proteins taking into account or neglecting the −2 charge of the PDX iron−sulfur cluster. Such an important role for the electrostatic attraction has been pointed out by previous experimental work[43] and docking studies.[17] Figures 1 and S1 (Supporting Information) clearly indicate that the electrostatic forces are crucial for the protein−protein recognition and binding. When neglecting the iron−sulfur negative charge, PDX binds to different regions

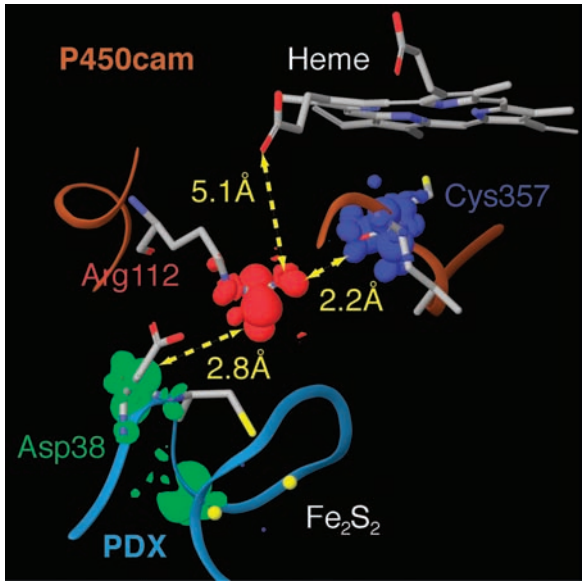

Figure 5. Electron transfer pathway for complex 4 of P450-PDX including the carbonyl group of Asp38 (PDX), the side chain of Arg112 (P450) and the carbonyl group of Cys357 (P450).

of the P450 surface. When including the correct active site charges, however, there is only one main binding area located in the heme proximal face. Thus, our results confirm the important role of the electrostatic attraction in the P450-PDX recognition.

Our calculations result in different electron transfer pathways for structures with different geometry, in agreement to other studies.[44] Complex 1, 3 and 4 are similar to earlier proposed complexes[16−18] having salt bridges between Arg112 (P450) and Asp38 (PDX) and iron−iron distances of around 13 Å. In complex 2, PDX is rotated around the vertical axis, avoiding the Arg112-Asp38 salt bridge, but still having an iron−iron distance of 14.2 Å. This structure has some similarity to the second proposed docking complex by Karyakin et al., which also has a rotation of PDX.

The electron transfer pathways obtained from the four protein−protein complexes indicate the important role of Arg112, in agreement with most previous mutational[19,20,45] and NMR studies.[16,46] In all four pathways the carbonyl groups acting as intermediates in the electron transfer are in the vicinity of this arginine. Furthermore, in complex 3 and 4 the side chain of Arg112 is directly involved in the pathway. For these two complexes, there is a larger direct ionic interaction between Arg112 and Asp38. Additionally, there is a weaker ionic interaction with the heme propionates. Actually, Arg112 experiences a larger rearrangement in complexes 3 and 4 in contrast to complexes 1 and 2. This can easily be seen by comparing the Arg112 distance to the heme propionate, having 2.8, 2.8, 4.5, and 5.1 Å for all four complexes, respectively. The change in the propionate environment has been observed by FTIR experiments.[18] Moreover, as seen in all pathway figures, the paths connect directly to Cys357. Thus, it seems like there is no direct involvement of the propionate groups in the electron delivery into the heme iron, in agreement with recent experimental work by Harada et al.[23]

Asp38 has also been pointed out as possible electron transfer mediator.[46,47] As seen in Figures 2, 4 and 5, in complexes 1, 3 and 4 the carbonyl group of this residue is directly involved in the electron transfer pathway. Thus, as indicated in previous studies, the pair Arg112−Asp38 seems to be a key player in the electron migration. Here we provide the first evidence using robust ab initio methodology for the involvement of these two residues. The only complex that does not involve Asp38 in the electron transfer pathway is complex 2. This structure presents a large rotation of the PDX, with respect to the other three complexes, placing Asp38 farther away from the interface. For this structure, the electron pathway deviates slightly from the more direct interface and the electron migration moves closer to the solvent. Upon close inspection of the coordinates we observed the presence of Arg109 in close vicinity to the electron pathway. We have recalculated the pathway after neutralizing this arginine and observed a substantial change in the electron migration. The new pathway, shown in red dashed lines in Figure 3, is substantially shorter, more buried in the protein−protein interface and involves now the side chain of Arg112. Thus, the proposed methodology is suitable for detecting variations in the electrostatic environment that might affect the electron transfer pathway, for example due to conformational dynamics.[44] Considering that calculations for a medium size region, of approximately 300 QM atoms, can be performed in 3−4 days using 8 SGI-Altix processors, the method appears as a great tool for analyzing several snapshots obtained from a conformational search, such as molecular dynamics.

In the absence of an experimental structure for the protein−protein complex, it is desirable to develop theoretical methods capable of producing bound structures and of analyzing the electron transfer pathway between them. The active role of Arg112 and Asp38, together with the larger rearrangement of the heme propionate vicinity, indicates that complexes 3 and 4 are in better agreement with previous experimental observations and constitute our best models for the protein−protein bound structure.

V. Conclusions

Here we present docking and ab initio QM studies for the electron transfer pathway between cytochrome P450camphor and putidaredoxin. The docking studies, in agreement with previous work, confirm the important role of the electrostatic forces in the protein−protein recognition and binding. The electron transfer pathway, obtained by means of a novel iterative ab initio QM procedure, indicates the key role of Arg112 and Asp38. The pathway connects directly PDX with the axial heme residue, Cys357. With the current computational resources, the methodology presented here appears as a promising tool to analyze the electron transfer pathways for a large ensemble of conformations.

Acknowledgment. Computational resources were provided by the Barcelona Supercomputing Center. Work was supported by startup funds from the Barcelona Supercomputer Center and by the Spanish Ministry of Education and Science through the project CTQ2007-62122/BQU.

Supporting Information Available: Figure of P450/PDX docking when neglecting the charge in the active site of PDX. Figures showing spin density plots for QM/MM spin density validation.This material is available free of charge via the Internet at http://pubs.acs.org.

References and Notes

(1) Beratan, D. N.; Onuchic, J. N.; Winkler, J. R.; Gray, H. B. *Science* **1992**, *258*, 1740.

(2) Langen, R.; Chang, I. J.; Germanas, J. P.; Richards, J. H.; Winkler, J. R.; Gray, H. B. *Science* **1995**, *268*, 1733.

(3) Kurnikov, I. V., *Department of Chemistry*; University of Pittsburgh: Pittsburgh, PA, 2000.
(4) Balabin, I. A.; Onuchic, J. *Science* **2000**, *290*, 114.
(5) Balabin, I. A.; Onuchic, J. N. *J. Phys. Chem.* **1996**, *100*, 11573.
(6) Gehlen, J. N.; Daizadeh, I.; Stuchebrukhov, A. A.; Marcus, R. A. *Inorg. Chim. Acta* **1996**, *243*, 271.
(7) Skourtis, S. S.; Beratan, D. N. *J. Phys. Chem. B* **1997**, *101*, 1215.
(8) Gruschus, J. M.; Kuki, A. *J. Phys. Chem. B* **1999**, *103*, 11407.
(9) Improta, R.; Barone, V.; Newton, M. D. *ChemPhysChem* **2006**, *7*, 1211.
(10) Migliore, A.; Corni, S.; Di Felice, R.; Molinari, E. *J. Chem. Phys.* **2006**, *124*, 064501.
(11) Ortiz de Montellano, P. *Cytochrome P450: Structure, Mechanism and Biochemistry*, 2nd ed.; Plenum: New York, 1995.
(12) Ogliaro, F.; Harris, N.; Cohen, S.; Filatov, M.; De Visser, S. P.; Shaik, S. *J. Am. Chem. Soc.* **2000**, *122*, 8977.
(13) Gunsalus, I. C.; Meeks, J. R.; Lipscomb, J. D.; Debrunner, P.; Munck, E. *Molecular Mechanisms of Oxygen Activation*; Academic Press: New York, 1974; p 559.
(14) Lewis, D. F. V. *Guide to Cytochrome P450: Structure and Function*; Taylor & Francis Ltd.: London, 1996.
(15) Brazeau, B. J.; Wallar, B. J.; Lipscomb, J. D. *Biochem. Biophys. Res. Commun.* **2003**, *312*, 143.
(16) Pochapsky, T. C.; Lyons, T. A.; Kazanis, S.; Arakaki, T.; Ratnaswamy, G. *Biochimie* **1996**, *78*, 723.
(17) Roitberg, A. E.; Holden, M. J.; Mayhew, M. P.; Kurnikov, I. V.; Beratan, D. N.; Vilker, V. L. *J. Am. Chem. Soc.* **1998**, *120*, 8927.
(18) Karyakin, A.; Motiejunas, D.; Wade, R. C.; Jung, C. *Biochim. Biophys. Acta (BBA) - Gen. Subj.* **2007**, *1770*, 420.
(19) Nakamura, K.; Horiuchi, T.; Yasukochi, T.; Sekimizu, K.; Hara, T.; Sagara, Y. *Biochim. Biophys. Acta* **1994**, *1207*, 40.
(20) Unno, M.; Shimada, H.; Toba, Y.; Makino, R.; Ishimura, Y. *J. Biol. Chem.* **1996**, *271*, 17869.
(21) Shimada, H.; Nagano, S.; Hori, H.; Ishimura, Y. *J. Inorg. Biochem.* **2001**, *83*, 255.
(22) Wade, R. C.; Motiejunas, D.; Schleinkofer, K.; Sudarko; Winn, P. J.; Banerjee, A.; Kariakin, A.; Jung, C. *Biochim. Biophys. Acta* **2005**, *1754*, 239.
(23) Harada, K.; Sakurai, K.; Ikemura, K.; Ogura, T.; Hirota, S.; Shimada, H.; Hayashi, T. *J. Am. Chem. Soc.* **2007**, *19*, 19.
(24) Wallrapp, F.; Guallar, V. *J. R. Soc. Interface*, in press.
(25) Jacobson, M. P.; Friesner, R. A.; Xiang, Z. X.; Honig, B. *J. Mol. Biol.* **2002**, *320*, 597.
(26) Jacobson, M. P.; Kaminski, G. A.; Friesner, R. A.; Rapp, C. S. *J. Phys. Chem. B* **2002**, *106*, 11673.
(27) Zheng, J.; Wang, D.; Thiel, W.; Shaik, S. *J. Am. Chem. Soc.* **2006**, *128*, 13204.
(28) Zurek, J.; Foloppe, N.; Harvey, J. N.; Mulholland, A. J. *Org. Biomol. Chem.* **2006**, *4*, 3931.
(29) Guallar, V.; Olsen, B. *J. Inorg. Biochem.* **2006**, *100*, 755.
(30) Cheng, T. M.-K.; Blundell, T. L.; Fernandez-Recio, J. *Proteins* **2007**, *68*, 503.
(31) Gabb, H. A.; Jackson, R. M.; Sternberg, M. J. *J. Mol. Biol.* **1997**, *272*, 106.
(32) Borrelli, K. W.; Vitalis, A.; Alcantara, R.; Guallar, V. *J. Chem. Theory Comput.* **2005**, *1*, 1304.
(33) Jacobson, M. P.; Pincus, D. L.; Rapp, C. S.; Honig, B.; Friesner, R. A. *Proteins* **2004**, *55*, 351.
(34) Bahar, I.; Atilgan, A. R.; Erman, B. *Folding Design* **1997**, *2*, 173.
(35) Van Der Spoel, D.; Lindahl, E.; Hess, B.; Groenhof, G.; Mark, A. E.; Berendsen, H. J. C. *J. Comput. Chem.* **2005**, *26*, 1701.
(36) Mo, Y. R.; Gao, J. L. *J. Comput. Chem.* **2000**, *21*, 1458.
(37) Reuter, N.; Dejaegere, A.; Maigret, B.; Karplus, M. *J. Phys. Chem. A* **2000**, *104*, 1720.
(38) Vreven, T.; Morokuma, K.; Farkas, O.; Schlegel, H. B.; Frisch, M. J. *J. Comput. Chem.* **2003**, *24*, 760.
(39) Friesner, R. A.; Guallar, V. *Annu. Rev. Phys. Chem.* **2005**, 56.
(40) Senn, H. M.; Thiel, W. QM/MM methods for biological systems. In *Atomistic Approaches in Modern Biology: From Quantum Chemistry to Molecular Simulations*, 2007; Vol. 268; pp 173.
(41) *QSite*; Schrödinger, Inc., Portland, Oregon., 2001.
(42) Harvey, J. N.; Bathelt, C. M.; Mulholland, A. J. *J. Comput. Chem.* **2006**, *27*, 1352.
(43) Stayton, P. S.; Poulos, T. L.; Sligar, S. G. *Biochemistry* **1989**, *28*, 8201.
(44) Prytkova, T. R.; Kurnikov, I. V.; Beratan, D. N. *Science* **2007**, *315*, 622.
(45) Koga, H.; Sagara, Y.; Yaoi, T.; Tsujimura, M.; Nakamura, K.; Sekimizu, K.; Makino, R.; Shimada, H.; Ishimura, Y.; Yura, K. *FEBS Lett.* **1993**, *331*, 109.
(46) Aoki, M.; Ishimori, K.; Morishima, I. *Biochim. Biophys. Acta* **1998**, *1386*, 168.
(47) Holden, M.; Mayhew, M.; Bunk, D.; Roitberg, A.; Vilker, V. *J. Biol. Chem.* **1997**, *272*, 21720.

JP803538U